

Nucleon-nucleon cross sections in neutron-rich matter and isospin transport in heavy-ion reactions at intermediate energies

Bao-An Li¹ and Lie-Wen Chen^{2,3}

¹ *Department of Chemistry and Physics, P.O. Box 419,*

Arkansas State University, State University, Arkansas 72467-0419, USA

² *Institute of Theoretical Physics, Shanghai Jiao Tong University, Shanghai 200240, China*

³ *Center of Theoretical Nuclear Physics, National Laboratory of Heavy Ion Accelerator, Lanzhou 730000, China*

Abstract

Nucleon-nucleon (NN) cross sections are evaluated in neutron-rich matter using a scaling model according to nucleon effective masses. It is found that the in-medium NN cross sections are not only reduced but also have a different isospin dependence compared with the free-space ones. Because of the neutron-proton effective mass splitting the difference between nn and pp scattering cross sections increases with the increasing isospin asymmetry of the medium. Within the transport model IBUU04, the in-medium NN cross sections are found to influence significantly the isospin transport in heavy-ion reactions. With the in-medium NN cross sections, a symmetry energy of $E_{sym}(\rho) \approx 31.6(\rho/\rho_0)^{0.69}$ was found most acceptable compared with both the MSU isospin diffusion data and the presently acceptable neutron-skin thickness in ²⁰⁸Pb. The isospin dependent part $K_{asy}(\rho_0)$ of isobaric nuclear incompressibility was further narrowed down to -500 ± 50 MeV. The possibility of determining simultaneously the in-medium NN cross sections and the symmetry energy was also studied. The proton transverse flow, or even better the combined transverse flow of neutrons and protons, can be used as a

probe of the in-medium NN cross sections without much hindrance from the uncertainties of the symmetry energy.

PACS numbers: 25.70.-z, 25.75.Ld., 24.10.Lx

I. INTRODUCTION

The isospin dependence of in-medium nuclear effective interactions is important for understanding not only novel properties of exotic nuclei near drip lines but also many interesting questions in astrophysics [1–3]. Especially, it determines the symmetry energy $E_{\text{sym}}(\rho)$ term in the equation of state (EOS) of isospin asymmetric nuclear matter. The density-dependent symmetry energy itself is still poorly known but very important for both nuclear physics and astrophysics. Heavy-ion reactions induced by neutron-rich nuclei provide a unique opportunity to explore the isospin dependence of in-medium nuclear effective interactions, especially the symmetry energy, in a broad range of density. This is because the isospin degree of freedom plays an important role in heavy-ion collisions through both the nuclear EOS and the nucleon-nucleon (NN) scatterings [4,5]. In particular, the transport of isospin asymmetry between two colliding nuclei is expected to depend on both the symmetry potential and the in-medium NN cross sections. For instance, the drifting contribution to the isospin transport in a nearly equilibrium system is proportional to the product of the mean relaxation time τ_{np} and the isospin asymmetric force F_{np} [6]. While the τ_{np} is inversely proportional to the neutron-proton (np) scattering cross section σ_{np} [6], the F_{np} is directly related to the gradient of the symmetry potential. On the other hand, the collisional contribution to the isospin transport in non-equilibrium system is generally expected to be proportional to the np scattering cross section. Thus the isospin transport in heavy-ion reactions depends on both the long-range and the short-range parts of the isospin-dependent in-medium nuclear effective interactions, namely, the symmetry potential and the in-medium np scatterings cross sections. The former relates directly to the density dependence of the symmetry energy $E_{\text{sym}}(\rho)$. To extract information about $E_{\text{sym}}(\rho)$ has been one of the major goals of heavy-ion reactions induced by neutron-rich nuclei [4,5]. Among the potential probes proposed so far, the isospin transport has been found very useful for investigating the $E_{\text{sym}}(\rho)$ [6–8]. More specifically, using the isospin and momentum dependent transport model IBUU04 [9], a symmetry energy of the form $E_{\text{sym}}(\rho) \approx 32(\rho/\rho_0)^{1.1}$ was extracted

recently from the MSU data on isospin transport [8]. This conclusion, however, was drawn based on transport model calculations using the experimental free-space NN cross sections. In this work, we examine effects of the in-medium NN cross sections on isospin transport in heavy-ion collisions at intermediate energies. The in-medium NN cross sections are calculated within a scaling model according to the nucleon effective masses consistent with the nuclear mean field used in the transport model. It is found that the density dependence of symmetry energy extracted from the isospin transport data is altered significantly. The possibility of determining both the in-medium NN cross sections and the symmetry energy corresponding to the same underlying nuclear effective interactions is also discussed.

II. MOMENTUM DEPENDENCE OF THE MEAN FIELD AND NUCLEON EFFECTIVE MASSES IN NEUTRON-RICH MATTER

The single nucleon potential is one of the most important inputs to all transport models for nuclear reactions. Both the isovector (symmetry potential) and isoscalar parts of this potential should be momentum dependent due to the non-locality of strong interactions and the Pauli exchange effects in many-fermion systems. In the IBUU04 transport model [9], we use a single nucleon potential derived within the Hartree-Fock approach using a modified Gogny effective interaction (MDI) [11], i.e.,

$$\begin{aligned}
U(\rho, \delta, \vec{p}, \tau, x) = & A_u(x) \frac{\rho_{\tau'}}{\rho_0} + A_l(x) \frac{\rho_{\tau}}{\rho_0} \\
& + B \left(\frac{\rho}{\rho_0} \right)^{\sigma} (1 - x\delta^2) - 8\tau x \frac{B}{\sigma + 1} \frac{\rho^{\sigma-1}}{\rho_0^{\sigma}} \delta \rho_{\tau'} \\
& + \frac{2C_{\tau, \tau}}{\rho_0} \int d^3 p' \frac{f_{\tau}(\vec{r}, \vec{p}')}{1 + (\vec{p} - \vec{p}')^2 / \Lambda^2} \\
& + \frac{2C_{\tau, \tau'}}{\rho_0} \int d^3 p' \frac{f_{\tau'}(\vec{r}, \vec{p}')}{1 + (\vec{p} - \vec{p}')^2 / \Lambda^2}.
\end{aligned} \tag{1}$$

FIGURES

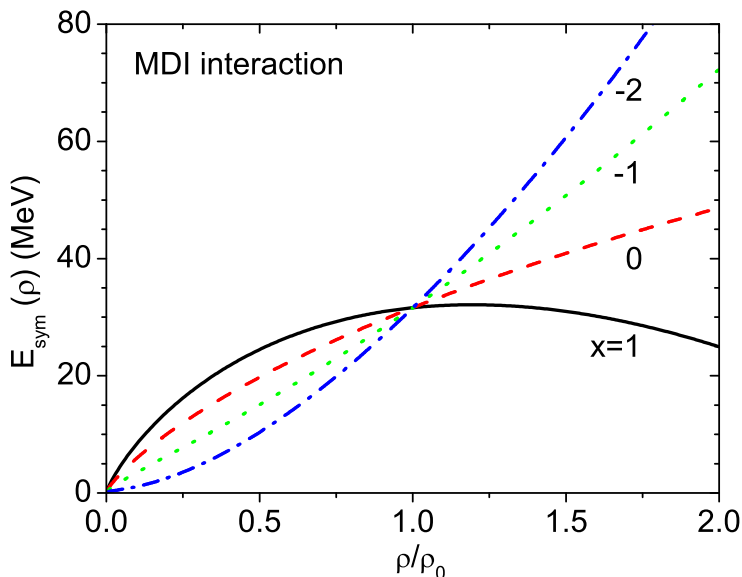


FIG. 1. (Color online) Symmetry energy as a function of density for the MDI interaction with $x = 1, 0, -1$ and -2 . Taken from ref. [8].

Here $\delta = (\rho_n - \rho_p)/\rho$ is the isospin asymmetry of the nuclear medium. In the above $\tau = 1/2$ ($-1/2$) for neutrons (protons) and $\tau \neq \tau'$; $\sigma = 4/3$; $f_\tau(\vec{r}, \vec{p})$ is the phase space distribution function at coordinate \vec{r} and momentum \vec{p} . The parameters $A_u(x), A_l(x), B, C_{\tau,\tau}, C_{\tau,\tau'}$ and Λ were obtained by fitting the momentum-dependence of the $U(\rho, \delta, \vec{p}, \tau, x)$ to that predicted by the Gogny Hartree-Fock and/or the Brueckner-Hartree-Fock (BHF) calculations [12], the saturation properties of symmetric nuclear matter and the symmetry energy of about 30 MeV at normal nuclear matter density $\rho_0 = 0.16 \text{ fm}^{-3}$ [11]. The incompressibility K_0 of symmetric nuclear matter at ρ_0 is set to be 211 MeV consistent with the latest conclusion from studying giant resonances [13–15]. The parameters $A_u(x)$ and $A_l(x)$ depend on the x parameter according to

$$A_u(x) = -95.98 - x \frac{2B}{\sigma + 1}, \quad A_l(x) = -120.57 + x \frac{2B}{\sigma + 1}. \quad (2)$$

The parameter x can be adjusted to mimic predictions on the density dependence of symmetry energy $E_{\text{sym}}(\rho)$ by microscopic and/or phenomenological many-body theories. Shown

in Fig. 1 is the density dependence of the symmetry energy for $x = -2, -1, 0$ and 1 . The last two terms in Eq. (1) contain the momentum-dependence of the single-particle potential. The momentum dependence of the symmetry potential stems from the different interaction strength parameters $C_{\tau,\tau'}$ and $C_{\tau,\tau}$ for a nucleon of isospin τ interacting, respectively, with unlike and like nucleons in the background fields. More specifically, we use $C_{unlike} = -103.4$ MeV and $C_{like} = -11.7$ MeV. With these parameters, the isoscalar potential estimated from $(U_{neutron} + U_{proton})/2$ agrees reasonably well with predictions from the variational many-body theory [16], the more advanced BHF approach [17] including three-body forces and the Dirac-Brueckner-Hartree-Fock (DBHF) calculations [18] in broad ranges of density and momentum.

What is particularly interesting and important for nuclear reactions induced by neutron-rich nuclei is the isovector (symmetry) potential. The strength of this potential can be estimated very accurately from $(U_{neutron} - U_{proton})/2\delta$ [9]. In Fig. 2 the strength of the symmetry potential for four x parameters is displayed as a function of momentum and density. Here we have only plotted the symmetry potential at sub-saturation densities most relevant to heavy-ion reactions studies at intermediate energies. It is noticed that the momentum dependence of the symmetry potential is independent of the parameter x . This is because the x appears only in the density dependent part of the single nucleon potential of Eq. (1) by construction. Systematic analyses of a large number of nucleon-nucleus scattering experiments and (p,n) charge exchange reactions at beam energies below about 100 MeV indicate undoubtedly that the symmetry potential at ρ_0 , i.e., the Lane potential, decreases approximately linearly with increasing beam energy E_{kin} . The data can be well described by using $U_{Lane} = a - bE_{kin}$ where $a \simeq 22 - 34$ MeV and $b \simeq 0.1 - 0.2$ [19–22]. One should comment that although the uncertainties in both the parameters a and b are large, the decreasing feature of the Lane potential with increasing beam energy is very certain. This provides a stringent constraint on the symmetry potential. The potential in Eq. (1) at ρ_0 satisfies this requirement very well as seen in Fig. 2. What is very uncertain but most interesting is the momentum-dependent symmetry potential at abnormal densities.

The experimental determination of both the density and momentum dependence of the symmetry potential is thus desired. Heavy-ion reactions provide a unique tool in terrestrial laboratories to explore the symmetry potential at abnormal densities with varying momenta.

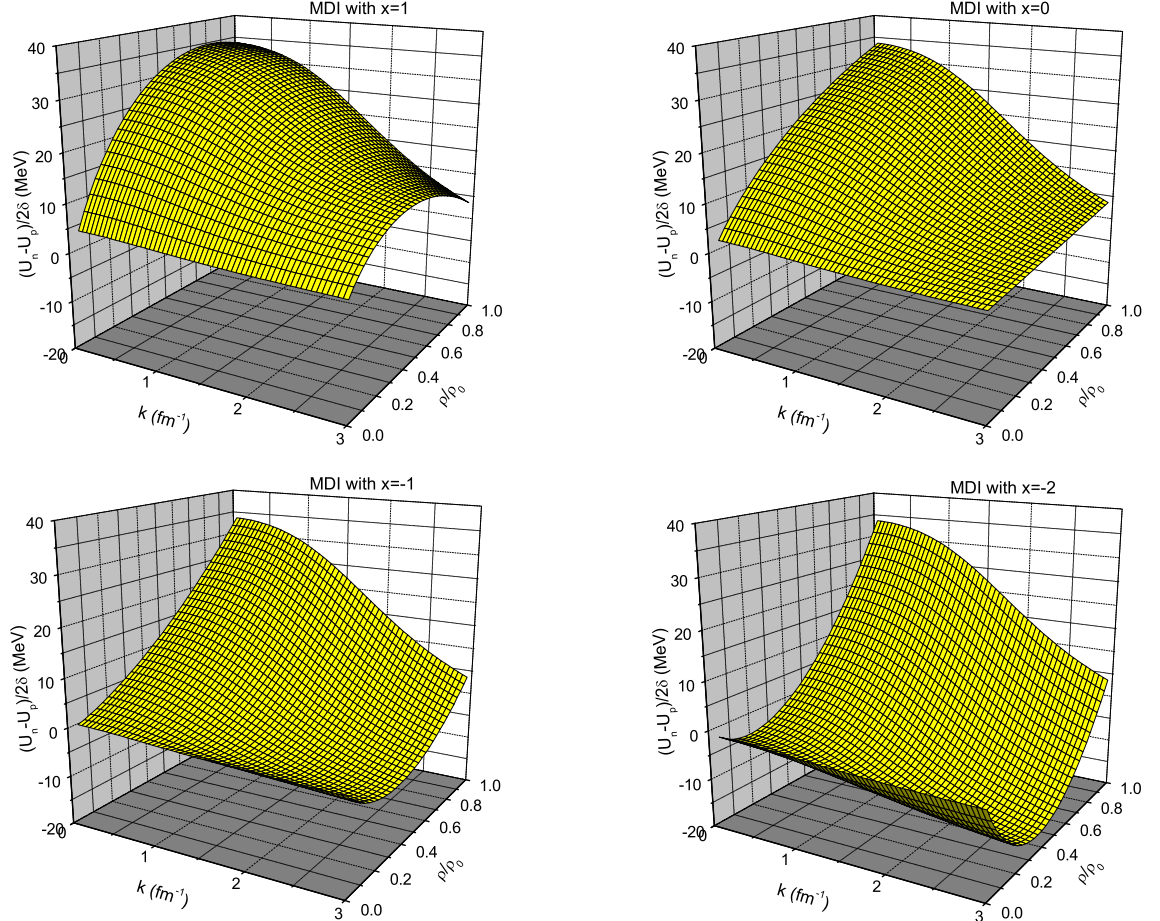


FIG. 2. (Color online) Symmetry potential as a function of momentum and density for MDI interactions with $x = 1, 0, -1$ and -2 .

One characteristic feature of the momentum dependence of the symmetry potential is the different effective masses for neutrons and protons in isospin asymmetric nuclear matter, i.e.,

$$\frac{m_\tau^*}{m_\tau} = \left\{ 1 + \frac{m_\tau}{p} \frac{dU_\tau}{dp} \right\}. \quad (3)$$

By definition, the effective mass normally depends on the density and isospin asymmetry of the medium as well as the momentum of the nucleon. Conventionally, however, the effective mass at the Fermi momentum $p_\tau = p_f(\tau)$ is most frequently used to characterize the momentum dependence of the nuclear potential. In our calculations of the in-medium NN cross sections, we use the general definition of Eq. (3). With the potential in Eq. (1), since the momentum-dependent part of the nuclear potential is independent of the parameter x , the nucleon effective masses are independent of the x parameter too.

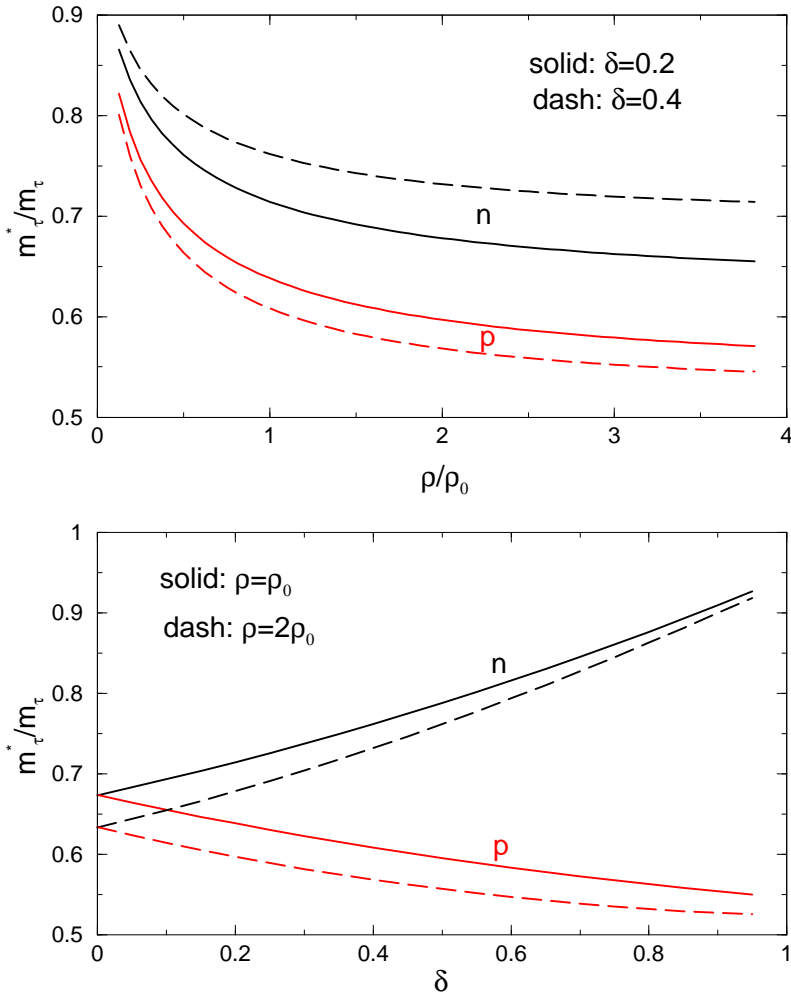


FIG. 3. (Color online) Nucleon effective masses at the respective Fermi surface in asymmetric matter as a function of density (upper window) and isospin asymmetry (lower window).

Shown in Fig. 3 are the effective masses of neutrons and protons at their respective Fermi surfaces as a function of density (upper window) and isospin asymmetry (lower window). It is seen that the effective mass of neutrons is higher than that of protons and the splitting between them increases with both the density and isospin asymmetry of the medium. We notice here that the momentum dependence of the symmetry potential and the associated neutron-proton effective mass splitting is still highly controversial within different approaches and/or using different nuclear effective interactions [23–25]. Being phenomenological and non-relativistic in nature the neutron-proton effective mass splitting in the present study is consistent with predictions of all non-relativistic microscopic models, see, e.g., [12,17,26], and the non-relativistic limit of microscopic relativistic many-body theories, see, e.g., [18,27,28]. Recent transport model studies indicate that the neutron/proton ratio at high transverse momenta and/or rapidities is a potentially useful probe of the neutron-proton effective mass splitting in neutron-rich matter [9,29]. In this work we explore effects of the neutron-proton effective mass splitting on in-medium NN cross sections in neutron-rich matter. Applications of these in-medium NN cross sections in heavy-ion reactions may be useful for finding other probes of the nucleon effective masses in neutron-rich matter.

III. NUCLEON-NUCLEON CROSS SECTIONS IN NEUTRON-RICH MATTER

While much attention has been given to finding experimental observables constraining the symmetry energy, little effort has been made so far to study the NN cross sections in isospin asymmetric nuclear matter. Most of the existing work on the in-medium NN cross sections have concentrated on their density dependence in isospin symmetric nuclear matter, see, e.g., [30–39]. Here we extend the effective mass scaling model for in-medium NN cross sections [30,31,34] to isospin asymmetric matter. Both the incoming current in the initial state and the level density of the final state in NN scatterings depend on the effective masses of the colliding nucleons. Assuming all matrix elements of the NN interactions are the same in free-space and in the medium, the NN cross sections in the medium σ_{NN}^{medium} are expected

to be reduced compared with their free-space values σ_{NN}^{free} by a factor

$$R_{medium} \equiv \sigma_{NN}^{medium} / \sigma_{NN}^{free} = (\mu_{NN}^* / \mu_{NN})^2, \quad (4)$$

where the μ_{NN} and μ_{NN}^* are the reduced masses of the colliding nucleon pairs in free-space and in the medium, respectively.

At relative momenta less than about 240 MeV/c and densities less than about $2\rho_0$, the scaling of $\sigma_{NN}^{medium} / \sigma_{NN}^{free}$ in Eq. (4) was recently found to be consistent with calculations based on the DBHF theory [40]. This finding lends a strong support to the effective mass scaling model of the in-medium NN cross sections in the limited density and momentum ranges. In this work, we apply the scaling model to elastic NN scatterings in heavy-ion reactions at beam energies up to about the pion production threshold. At higher energies, inelastic reaction channels become important and in-medium effects on these channels have been a subject of much interest, see, e.g., refs. [41–43]. For the inelastic channels we keep using the experimental free-space cross sections. This assumption has no effect on our present study mainly at intermediate energies.

While the effective masses and the in-medium NN cross sections have to be calculated dynamically in the evolving environment created during heavy-ion reactions, it is instructive to examine the in-medium NN cross sections in isospin asymmetric nuclear matter at zero temperature. In this situation the integrals in Eq. (1) can be analytically carried out. More specifically [11,44],

$$\int d^3p' \frac{f_\tau(\vec{r}, \vec{p}')}{1 + (\vec{p} - \vec{p}')^2 / \Lambda^2} = \frac{2}{h^3} \pi \Lambda^3 \left[\frac{p_f^2(\tau) + \Lambda^2 - p^2}{2p\Lambda} \ln \frac{(p + p_f(\tau))^2 + \Lambda^2}{(p - p_f(\tau))^2 + \Lambda^2} + \frac{2p_f(\tau)}{\Lambda} - 2 \left\{ \arctan \frac{p + p_f(\tau)}{\Lambda} - \arctan \frac{p - p_f(\tau)}{\Lambda} \right\} \right]. \quad (5)$$

The medium reduction factor R_{medium} can thus also be obtained analytically, albeit lengthy.

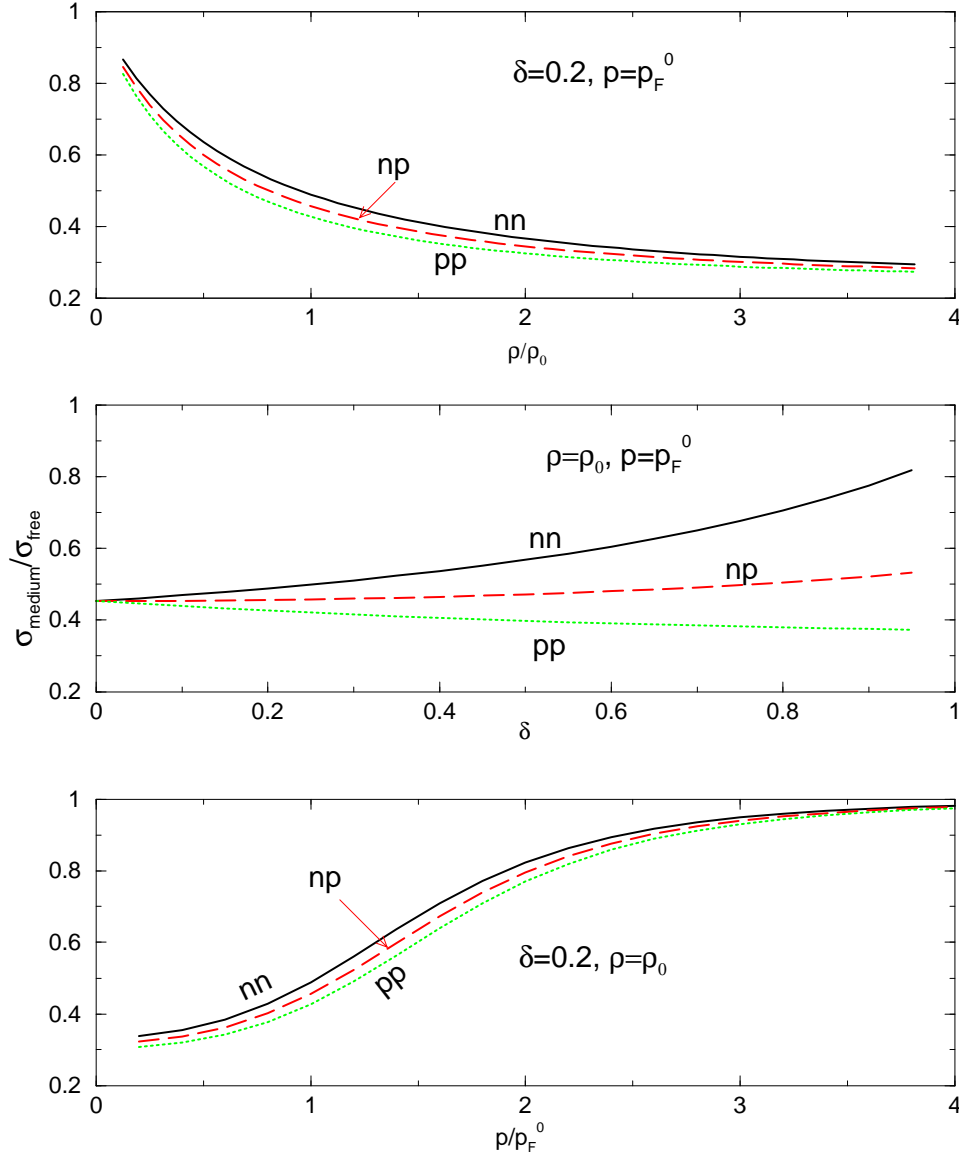


FIG. 4. (Color online) The reduction factor of the in-medium nucleon-nucleon cross sections compared to their free-space values as a function of density (top), isospin asymmetry (middle) and momentum (bottom).

As an illustration of a simplified case, we show in Fig. 4 the reduction factor R_{medium} for two colliding nucleons having the same momentum p . The R_{medium} factor is examined as a function of density (upper), isospin asymmetry (middle) and the momentum (bottom). It is interesting to note that the in-medium NN cross sections are not only reduced compared with

their free-space values, but the nn and pp cross sections are also split while their free-space cross sections are the same. Moreover, the difference between the nn and pp scattering cross sections grows in more asymmetric matter. The higher in-medium cross sections for nn than for pp are completely due to the positive neutron-proton effective mass splitting with the effective interaction used. This feature may serve as a probe of the neutron-proton effective mass splitting in neutron-rich matter. This possibility will be studied in a future work. We also note that the in-medium NN cross sections are also independent of the parameter x . They are solely determined by the momentum dependence of the nuclear potential used in the model.

IV. DYNAMICAL GENERATION OF NUCLEON EFFECTIVE MASSES DURING HEAVY-ION REACTIONS

The nucleon effective masses change dynamically in heavy-ion collisions. How big are the nucleon effective masses and how much the NN cross sections are modified compared with their free-space values in a typical heavy-ion reaction at intermediate energies? To answer these questions, we show in Fig. 5 the correlation between the average nucleon effective mass and the average nucleon density (top), and the distribution of nucleon effective masses (bottom) at the instant of 10 fm/c in the reaction of $^{132}\text{Sn}+^{124}\text{Sn}$ at a beam energy of 50 MeV/A and an impact parameter of 5 fm. For this particular calculation $x = 0$ is used, very similar results are obtained using other values for the x parameter. It is seen that the nucleon effective masses decrease with increasing density. The maximum density reached at the instant considered, i.e., 10 fm/c, is about $1.4\rho/\rho_0$. Moreover, the neutron-proton effective mass splitting is seen to increase slightly at supra-normal densities. However, the increase is not much because the isospin asymmetry normally decreases with increasing density, i.e., the isospin fractionation (distillation), see, e.g., [4,5,55]. These features are consistent with our expectations discussed in previous sections. From the lower window it is seen that the distribution of nucleon effective masses picks at about 0.7 GeV. It is also

noticed that some small number of nucleons obtain effective masses above their free masses. This is also understandable. In principle, the slope of the nucleon potential du/dp in Eq. (3) can be negative during heavy-ion reactions although it happens very rarely, leading to the higher effective masses of some nucleons.

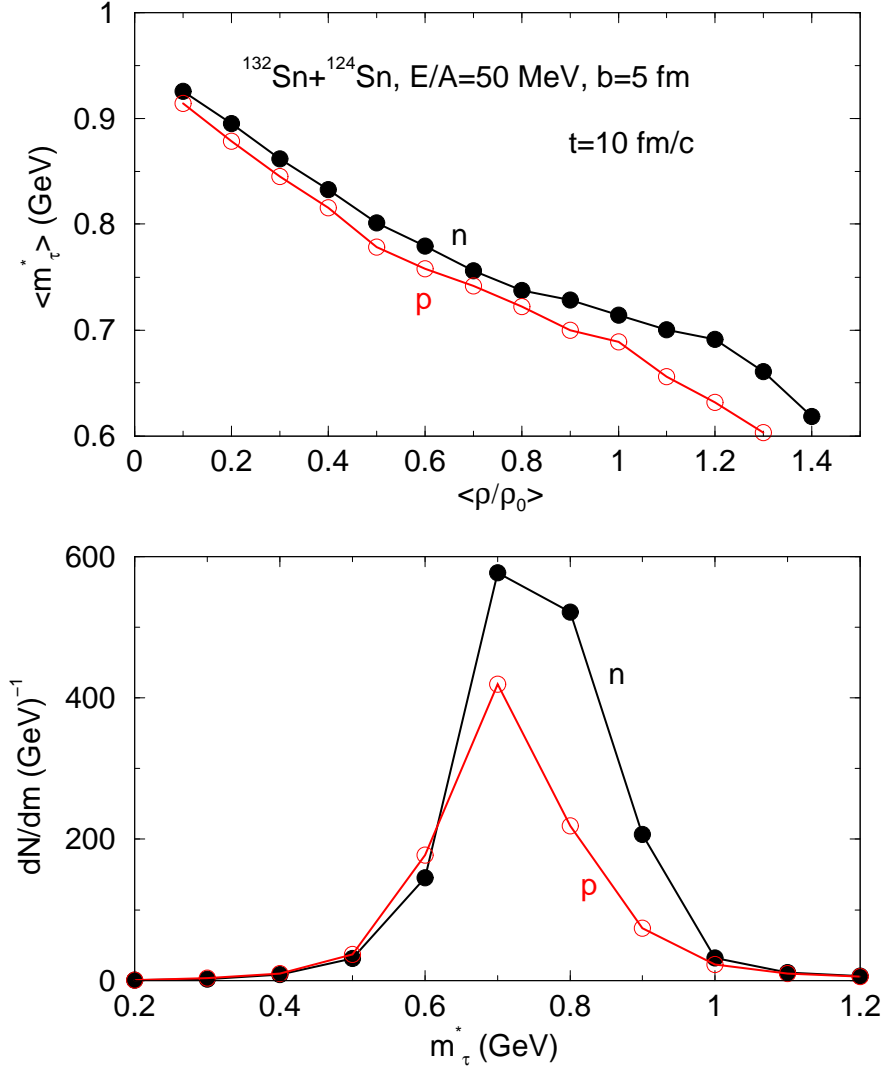


FIG. 5. (Color online) The correlation between the average nucleon effective mass and the average nucleon density (top), and the distribution of nucleon effective masses (bottom) in the reaction of $^{132}\text{Sn}+^{124}\text{Sn}$ at a beam energy of 50 MeV/A and an impact parameter of 5fm.

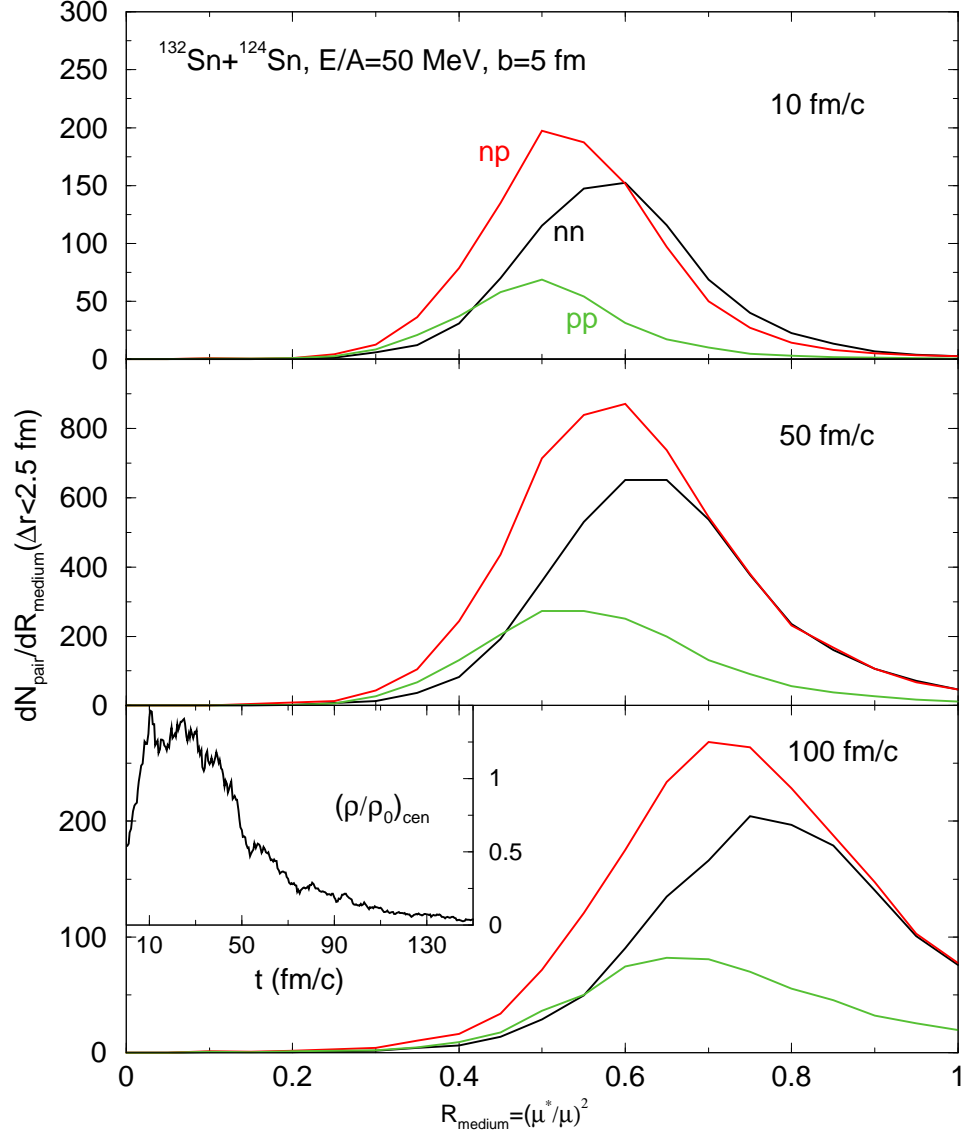


FIG. 6. (Color online) The distribution of the reduction factor of in-medium NN cross sections in the reaction of $^{132}\text{Sn}+^{124}\text{Sn}$ at a beam energy of 50 MeV/A and an impact parameter of 5fm at 10, 50 and 100 fm/c, respectively. The insert is the evolution of the central density in the reaction.

With the nucleon effective masses available we can now examine their effects on nucleon-nucleon scatterings during heavy-ion reactions. Shown in Fig. 6 are the distributions of the reduction factor R_{medium} in the reaction of $^{132}\text{Sn}+^{124}\text{Sn}$ at a beam energy of 50 MeV/A and

an impact parameter of 5 fm at 10, 50 and 100 fm/c, respectively. The insert in the bottom window shows the evolution of the central density during the reaction. The three instants represent the compression, expansion and freeze-out stages of the reaction. The quantity $N_{pair}(\Delta r < 2.5 fm)$ is the number of nucleon pairs with spatial separations less than 2.5 fm. These are potential colliding nucleons whose scattering cross section will be reduced by the factor R_{medium} , i.e., $\sigma_{NN}^{medium} = R_{medium} \times \sigma_{NN}^{free}$. It is seen that on average as much as 50% reduction occurs for NN scatterings in the early stage of the reaction. As the system expands the average density decreases, the reduction factor R_{medium} thus gradually shifts towards 1 in the later stage of the reaction.

V. EFFECTS OF THE IN-MEDIUM NN CROSS SECTIONS ON ISOSPIN TRANSPORT IN HEAVY-ION REACTIONS AT INTERMEDIATE ENERGIES

The in-medium NN cross sections are expected to affect several aspects of heavy-ion reactions. Previous studies have already found that the in-medium NN cross sections influence both the degree and rate of isospin equilibrium [45–50], see, e.g., [51] for a review. However, none of them is in the context of extracting the symmetry energy. In this section we investigate how the symmetry energy extracted from the isospin transport data might be altered.

A. Isospin diffusion/transport

Experimentally, one way of measuring quantitatively the amount of isospin transport, between the projectile nucleus A and the target nucleus B is to study the quantity R_i defined as [52]

$$R_i = \frac{2X^{A+B} - X^{A+A} - X^{B+B}}{X^{A+A} - X^{B+B}} \quad (6)$$

where X is any isospin-sensitive observable. The R_i is also known as a useful tool of measuring quantitatively the degree of isospin diffusion in heavy-ion reactions [7]. Here we prefer to

use the more general term isospin transport although the two terminologies may have been used interchangeably in the literature. Our main concern is that the term diffusion is often associated with irreversible processes. While by definition as given in Eq. (6), and from analyzing its time evolution in the following, it is seen that the R_i does not always have to decrease with time. In other words, there is no guarantee that the particular observable X is synchronized in all three reaction systems such that R_i always decreases with time. This is because the evolution and freeze-out time of the observable X may depend significantly on the system size especially if the masses of A and B are rather different. By construction, the value of R_i is 1 (-1) for the symmetric $A + A$ ($B + B$) reaction. If an isospin equilibrium is reached as a result of isospin transport the value of R_i is about zero. As mentioned earlier, the EOS of symmetric nuclear matter still has some uncertainties associated with the density and momentum dependence of the isoscalar potential. Fortunately, these uncertainties and all others due to the isospin-independent ingredients in the reaction dynamics can be largely canceled out because of the special construction of R_i . The R_i also has the advantage of minimizing significantly effects of pre-equilibrium emissions [7].

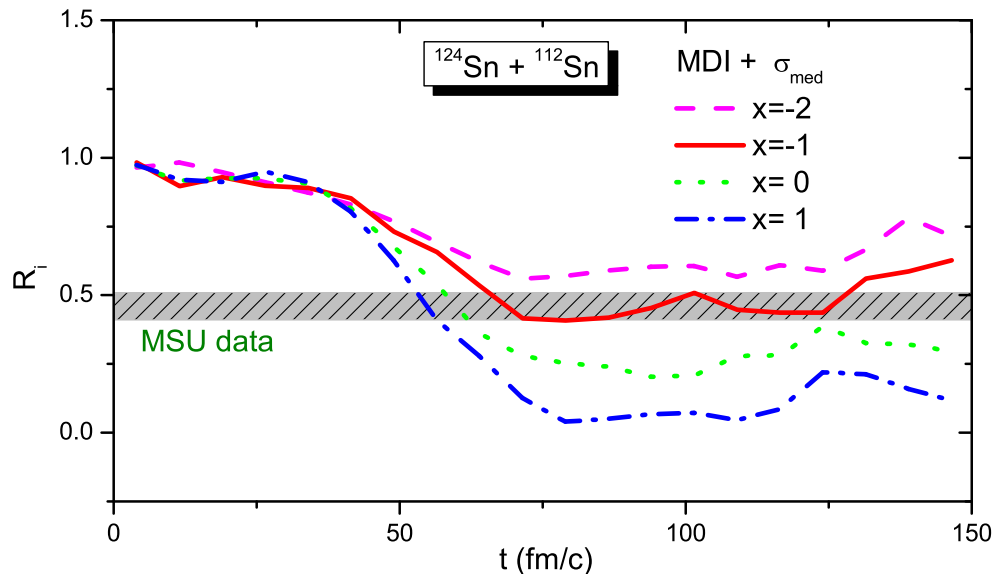


FIG. 7. (Color online) The evolution of isospin diffusion R_i using the four x parameters and the in-medium nucleon-nucleon cross sections.

In the NSCL/MSU experiments with $A = {}^{124}\text{Sn}$ on $B = {}^{112}\text{Sn}$ at a beam energy of 50 MeV/nucleon and an impact parameter about 6 fm, the isospin asymmetry of the projectile-like residue was used as the isospin tracer X [7]. The data was recently analyzed within the IBUU04 transport model using the free-space experimental NN cross sections. Consistent with the experimental selection, in model analyses the average isospin asymmetry $\langle\delta\rangle$ of the ${}^{124}\text{Sn}$ -like residue was calculated from nucleons with local densities higher than $\rho_0/20$ and velocities larger than 1/2 the beam velocity in the c.m. frame. Shown in Fig. 7 are the time evolutions of R_i re-calculated using the in-medium NN cross sections and the four x parameters. The data from MSU is indicated by the shaded band. It is seen that the net isospin transport and the influence of the x parameter show up mainly in the expansion phase of the reaction after about 40 fm/c. The values of R_i stabilize approximately after about 80 fm/c. It is seen that the values of R_i with $x = -1$ and 0 come close to the MSU data in the late stage of the reaction.

For a more meaningful comparison with the experimental data, we have calculated the time average of R_i between $t = 120$ fm/c and 150 fm/c as in Ref. [8]. Shown in Fig. 8 is a comparison of the averaged strength of isospin transport $1 - R_i$ obtained with the free and in-medium NN cross sections, respectively, as a function of the asymmetric part of the isobaric incompressibility of nuclear matter at ρ_0 [53–55]

$$K_{\text{asy}}(\rho_0) \equiv 9\rho_0^2 \left(d^2 E_{\text{sym}}/d\rho^2 \right)_{\rho_0} - 18\rho_0 (dE_{\text{sym}}/d\rho)_{\rho_0}. \quad (7)$$

In each case, 2000 events were generated for all three reaction systems used in the analysis. The error bars were drawn to indicate fluctuations and were obtained from the dispersion of R_i time evolution [8]. First, it is interesting to note that with the in-medium NN cross sections the strength of isospin transport $1 - R_i$ decreases monotonically with the decreasing value of x . With the free-space NN cross sections, however, there appears to be a minimum at around $x = -1$. Moreover, this minimum is the point closest to the experimental data. This allowed us to extract the value of $K_{\text{asy}}(\rho_0) = -550 \pm 100$ MeV. With the in-medium NN cross sections we can now further narrow down the $K_{\text{asy}}(\rho_0)$ to be about -500 ± 50

MeV. The latter is consistent with that extracted from studying the isospin dependence of giant resonances of ^{112}Sn to ^{124}Sn isotopes by Fujiwara et al at Osaka [56]. Shown also in the figure are the γ values used in fitting the symmetry energy with $E_{\text{sym}}(\rho) = 31.6(\rho/\rho_0)^\gamma$. The results with the in-medium NN cross sections constrain the γ parameter to be between 0.69 and 1.05. The lower value is close to what is extracted from studying giant resonances [57,58]. The value of $\gamma = 1.05$ extracted earlier using the free-space NN cross sections sets an upper limit.

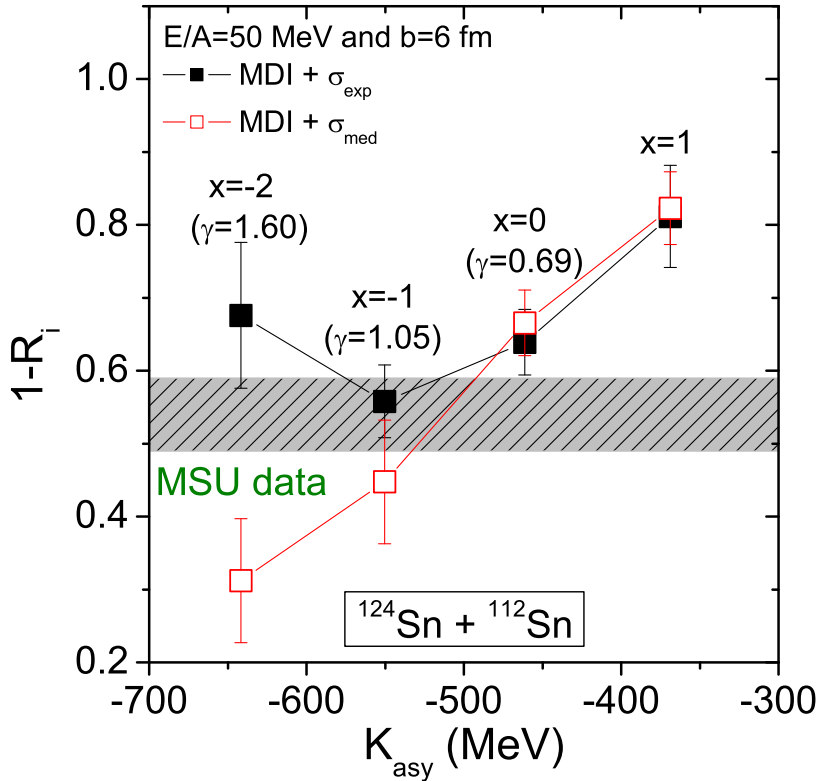


FIG. 8. (Color online) The degree of isospin transport as a function of $K_{\text{asy}}(\rho_0)$ with the free (filled squares) and in-medium (open squares) nucleon-nucleon cross sections.

It is seen that the difference in $1 - R_i$ obtained with the free-space and the in-medium NN cross sections is about the same with $x = 1$ and $x = 0$, but then becomes especially large at $x = -1$ and $x = -2$. Why does the effect of the in-medium NN cross sections increase with the decreasing $K_{\text{asy}}(\rho_0)$ or x parameter? This question can be understood from considering

contributions from the symmetry potential and the np scatterings. As we have mentioned in the introduction, both contributions to the isospin transport depend on the np scattering cross section σ_{np} . Schematically, the mean field contribution is proportional to the product of the isospin asymmetric force F_{np} and the inverse of the np scattering cross section σ_{np} . While the collisional contribution is proportional to the σ_{np} . The overall effect of the in-medium NN cross sections on isospin transport is a result of a complicated combination of both the mean field and the NN scatterings. Generally speaking, the symmetry potential effects on the isospin transport will become weaker when the NN cross sections are larger while the symmetry potential effects will show up more clearly if smaller NN cross sections are used. This feature can be seen from Fig. 9.

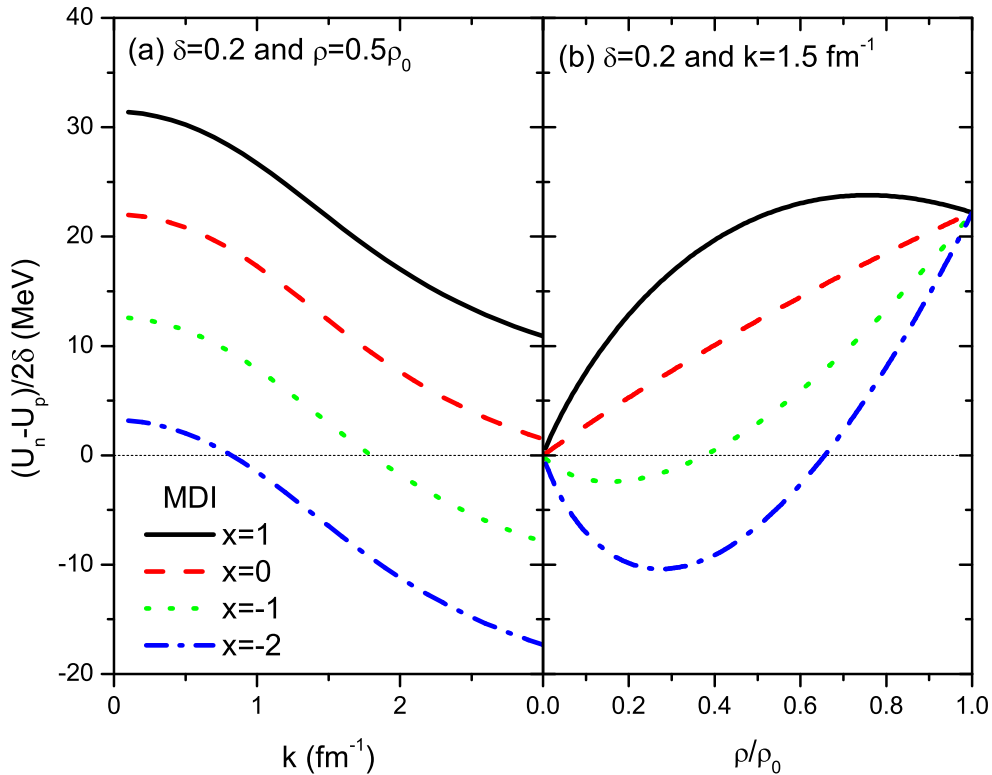


FIG. 9. (Color online) Symmetry potential as a function of momentum at selected densities (a), and density at selected momenta (b) with the four x parameters. Taken from Ref. [8].

For $x = 1$ and $x = 0$, the symmetry potential and its density slope, as shown in Fig. 9, are large at low densities where the majority of net isospin transport occurs. The F_{np} factor

makes the contribution due to the mean field dominates over that due to the collisions. Therefore, the reduced in-medium σ_{np} leads to about the same or a slightly higher isospin transport. As the x parameter decreases to $x = -1$ and $x = -2$, however, the symmetry potential decreases and its density slope can be even negative at low densities. Thus in these cases either the collisional contribution dominates or the mean field contribution becomes negative. The reduced in-medium np scattering cross section σ_{np} leads then to a lower isospin transport compared with the case with the free-space NN cross sections.

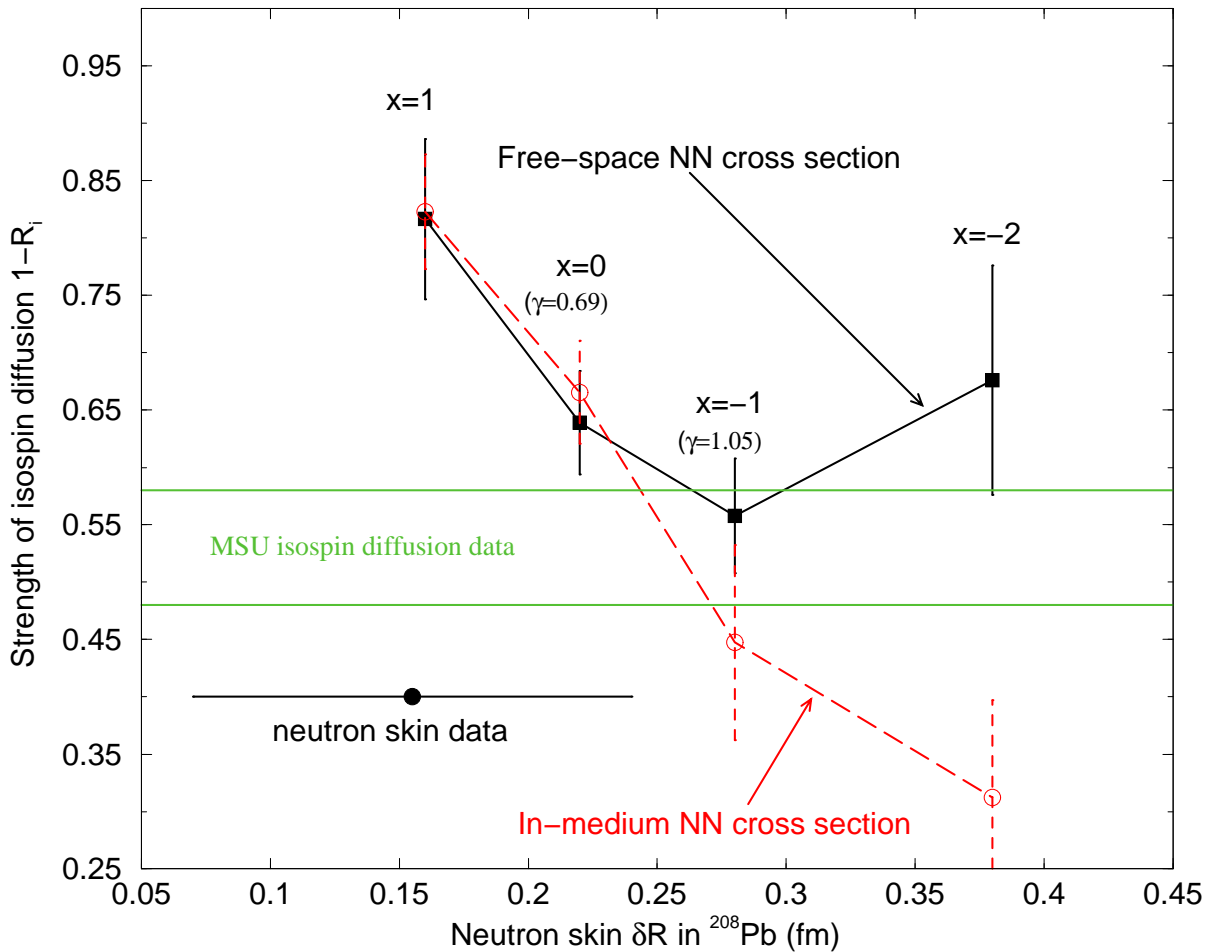


FIG. 10. (Color online) The skin thickness in lead, δR , versus the isospin diffusion parameter $1 - R_i$ for the four equations of state in this work. The present acceptable experimental range for δR and the NSCL/MSU data on isospin diffusion are also shown.

B. Correlation between the isospin diffusion and neutron-skin in ^{208}Pb

Both the neutron skin of heavy nuclei and the degree of isospin diffusion in heavy-ion collisions at intermediate energies are sensitive to the symmetry energy at sub-saturation densities. Since they both are determined by the same underlying EOS, the correlation between these seemingly very different observables provides a more stringent constraint on the symmetry energy than their individual values [59]. In view of the revised calculations of the isospin diffusion using the in-medium NN cross sections, here we revisit the correlation between the isospin diffusion and the size of neutron-skin in ^{208}Pb . Shown in Fig. 10 is the isospin diffusion parameter $1 - R_i$ versus the skin thickness in lead, δR . The presently acceptable experimental range for δR [60] and the NSCL/MSU data on isospin diffusion are also shown. The δR , taken from Ref. [59], was calculated within the Hartree-Fock approach using the same equations of state corresponding to the four x parameters. While the isospin diffusion data is between calculations with $x = 0$ and $x = -1$, the upper limit of the present n-skin measurements comes closer to the prediction using $x = 0$. On one hand, the present analysis of the isospin diffusion data favors a neutron skin as large as about 0.25 fm. On the other hand, the present neutron-skin data favors $x = 0$ and $x = 1$. One can thus conclude that a symmetry energy of $E_{\text{sym}}(\rho) \approx 31.6(\rho/\rho_0)^{0.69}$ is currently most acceptable based on both the neutron-skin and the isospin diffusion data. It is seen that more accurate measurements of both kinds of experimental data, especially the neutron-skin, are very desirable.

VI. NUCLEON TRANSVERSE FLOW AS A PROBE OF THE IN-MEDIUM NN CROSS SECTIONS

Our results above indicate clearly that the in-medium NN cross sections affect significantly the extraction of symmetry energy from isospin transport in heavy-ion reactions. Therefore, auxiliary measurements of other observables have to be made to constrain the

in-medium NN cross sections, preferably from the same experiments. Fortunately, a number of observables are known to be sensitive to the in-medium NN cross sections. These include the quadruple moment Q_{zz} of nucleon momentum distribution, the linear momentum transfer (LMT) and the ratio of transverse to longitudinal energies (ERAT), see, e.g., ref. [39,43,61,62]. It is also well known that these observables are also sensitive to the EOS of symmetric matter. Therefore, the extraction of the in-medium NN cross sections from these observables relies closely on our knowledge about the EOS of symmetric nuclear matter. Nevertheless, great progress has been made over the last three decades in determining the EOS of symmetric nuclear matter. Using a combination of several observables in heavy-ion reactions, such as the elliptic flow and kaon production, see, e.g., Refs. [63–65], and the analysis of giant resonances, the EOS of symmetric nuclear matter has been severely constrained. It has now been widely recognized that the major remaining uncertainty in further constraining the EOS of symmetric nuclear matter is our poor knowledge about the symmetry energy [14,15,64]. In this work we thus concentrate on the possibility of extracting the symmetry energy and the in-medium NN cross sections simultaneously without considering the remaining uncertainty in the EOS of symmetric matter.

In this work we choose to use the transverse flow to constrain the in-medium NN cross sections. Its sensitivity to variations of the in-medium NN cross sections is well known, especially around the balance energies, see, e.g., [66–73]. As an illustration, shown in Fig. 11 is the transverse flow of all free nucleons identified as those having local densities less than $\rho_0/8$ at freeze-out in the reaction of $^{132}\text{Sn}+^{124}\text{Sn}$ at an impact parameter of 5 fm and a beam energy of 400 MeV/A (upper) and 50 MeV/A (bottom) with the free-space and in-medium NN cross sections, respectively. It is seen that at 50 MeV/A the transverse flow is much more sensitive to the in-medium NN cross sections than at 400 MeV/A. In fact, the direction of transverse flow is altered from being positive to slightly negative by the reduced in-medium NN cross sections. This observation is consistent with our expectation and results of previous studies.

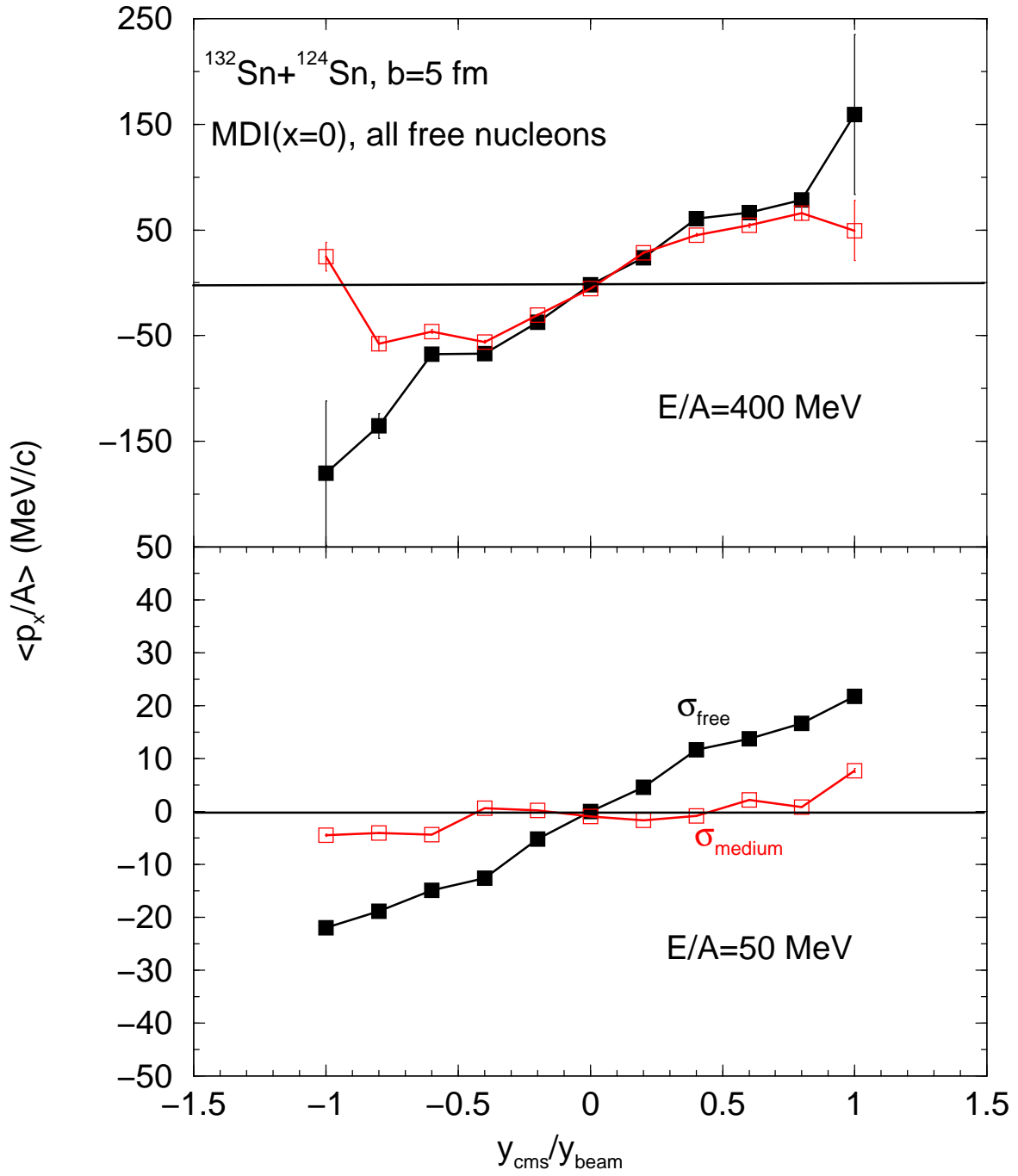


FIG. 11. Nucleon transverse flow in the reaction of $^{132}\text{Sn} + ^{124}\text{Sn}$ at an impact parameter of 5 fm and a beam energy of 400 MeV/A (upper) and 50 MeV/A (bottom).

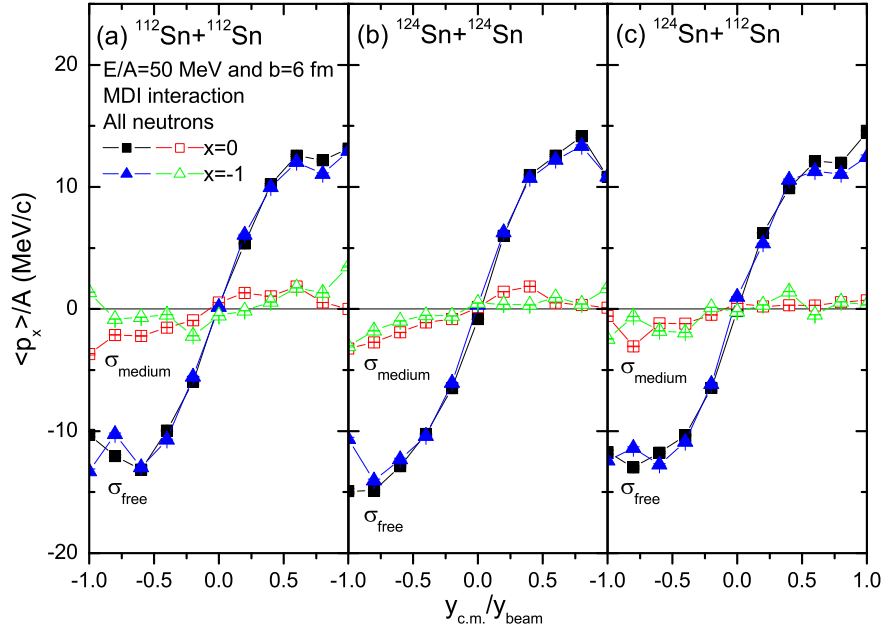


FIG. 12. Neutron transverse flow in the reaction of $^{112}\text{Sn} + ^{112}\text{Sn}$ (left), $^{124}\text{Sn} + ^{124}\text{Sn}$ (middle) and $^{124}\text{Sn} + ^{112}\text{Sn}$ (right) at an impact parameter of 6 fm and a beam energy of 50 MeV/A.

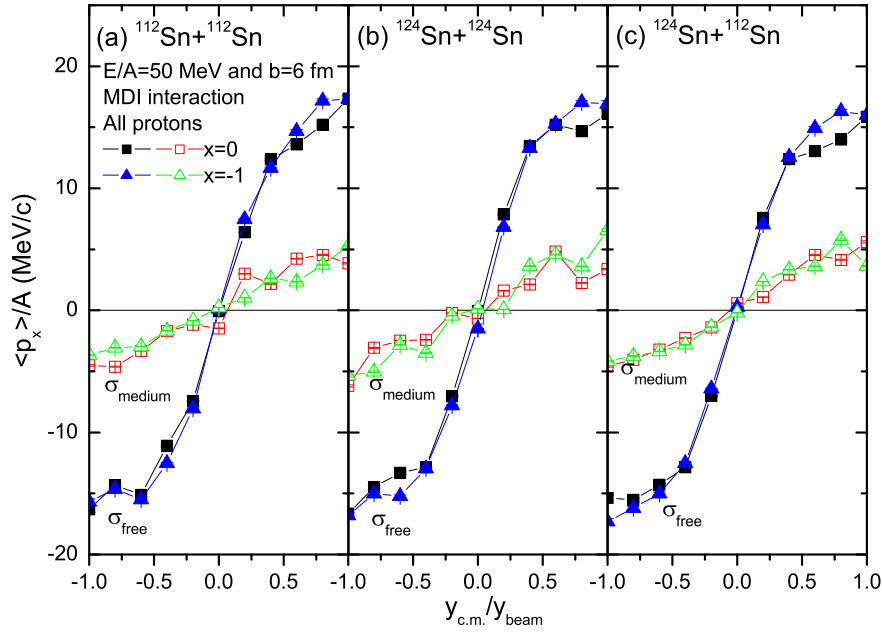


FIG. 13. Proton transverse flow in the reaction of $^{112}\text{Sn} + ^{112}\text{Sn}$ (left), $^{124}\text{Sn} + ^{124}\text{Sn}$ (middle) and $^{124}\text{Sn} + ^{112}\text{Sn}$ (right) at an impact parameter of 6 fm and a beam energy of 50 MeV/A.

Shown in Figs. 12 and 13 are the transverse flow for all (free and bound) neutrons and protons, respectively, with $x = 0$ and $x = -1$ for the three reactions used in studying the isospin transport. Free nucleons show the same features but with poor statistics for the same number of events. There is very little system size dependence among the three reactions considered. It is seen that the transverse flow is much more sensitive to the in-medium NN cross sections than to the symmetry energy parameter x . There is a weak sensitivity to the variation of the x parameter, especially with the reduced in-medium NN cross sections for neutrons. Protons are affected by both the repulsive Coulomb potential and the generally attractive symmetry potential, while neutrons are only affected by the repulsive symmetry potential, besides the same isoscalar potential acting on both neutrons and protons. Neutrons thus appear to be more sensitive to the x parameter. Moreover, the Coulomb potential dominates over the symmetry potential, leading to the slightly higher transverse flow for protons than for neutrons as seen from comparing Fig. 12 with Fig. 13. It is also interesting to note from comparing Fig. 12 with Fig. 13 that there is a clear indication of higher (lower) transverse flow for neutrons (protons) with $x = 0$ than that with $x = -1$, especially around the projectile and target rapidities. This feature is what one expects from considering the symmetry potentials shown in Fig. 9. At sub-saturation densities the symmetry potential is stronger with $x = 0$ than that with $x = -1$. Therefore, the neutron (proton) transverse flow is stronger (weaker) with $x = 0$. This fine dependence on the symmetry energy parameter x can be studied in more detail by using the neutron-proton differential flow [74]. We find, however, that the strength of the neutron-proton differential flow only changes by about 1 to 2 MeV/c by varying the x parameter from -1 to 0. It is much less than the change due to the variation of the in-medium NN cross sections. Based on these results, we therefore propose to measure the proton transverse flow in order to constrain the in-medium NN cross sections.

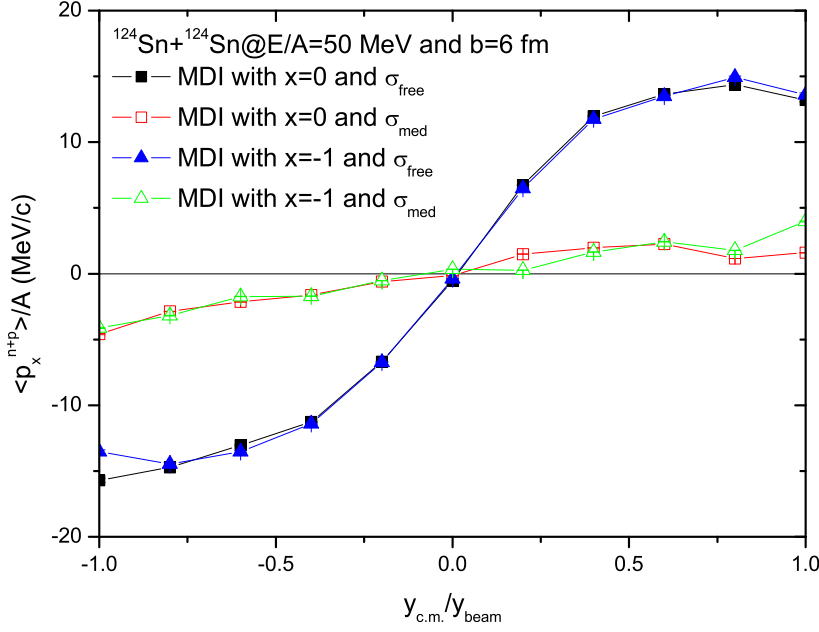


FIG. 14. Combined nucleon transverse flow in the reaction of $^{124}\text{Sn} + ^{124}\text{Sn}$ at an impact parameter of 6 fm and a beam energy of 50 MeV/A.

To go one step further, taking into account the generally positive/negative nature of the symmetry potentials for neutrons/protons, one may use the combined transverse flow of neutrons and protons $\langle p_x^{n+p} \rangle / A$ to better determine the in-medium NN cross sections without much influence of the symmetry potential. This, of course, requires measuring neutrons as accurately as protons simultaneously. Shown in Fig. 14, is an example of the combined nucleon flow for the $^{124}\text{Sn} + ^{124}\text{Sn}$ reactions. It is clearly seen that the combined flow of all nucleons are much less affected by the variation of the symmetry energy, making it an even better probe of the in-medium NN cross sections.

VII. SUMMARY

In order to better understand the isospin dependence of the in-medium nuclear effective interactions, we investigated effects of the in-medium NN cross sections on isospin transport in heavy-ion reactions within the transport model IBUU04. The isospin-dependent in-medium NN cross sections consistent with the nuclear mean field used in the transport

model were evaluated by using the scaling model according to the nucleon effective masses. It is found that the NN cross sections in neutron-rich matter are not only reduced compared with their values in free space, their isospin dependence is also altered. Because of the positive and growing neutron-proton effective mass splitting in more neutron-rich matter for the effective interactions used in this work, the splitting between the nn and pp cross sections increases with the increasing isospin asymmetry of the medium.

The in-medium NN cross sections are found to influence significantly the isospin transport and nucleon transverse flow in heavy-ion reactions at intermediate energies. By using the free-space experimental NN cross sections, a symmetry energy of $E_{\text{sym}}(\rho) \approx 31.6(\rho/\rho_0)^{1.1}$ was extracted from the MSU data on isospin transport. With the in-medium NN cross sections, however, the symmetry energy of $E_{\text{sym}}(\rho) \approx 31.6(\rho/\rho_0)^{0.69}$ was found most acceptable in comparison with both the MSU isospin diffusion data and the presently acceptable neutron-skin thickness in ^{208}Pb . The isospin dependent part $K_{\text{asy}}(\rho_0)$ of the isobaric incompressibility of nuclear matter was further narrowed down to -500 ± 50 MeV.

The possibility of determining simultaneously both the in-medium NN cross sections and the symmetry energy corresponding to the same underlying nuclear effective interactions was also studied. The proton transverse flow, or even better the combined transverse flow of neutrons and protons all together, can be used as an effective probe of the in-medium NN cross sections without much hindrance from the uncertainties of the symmetry energy. Our findings in this work demonstrated clearly the importance of using the in-medium NN cross sections consistent with the momentum-dependent nuclear mean field in transport model studies of heavy-ion reactions.

We would like to thank Dr. A.W. Steiner for helpful discussions. The work of B.A. Li is supported in part by the US National Science Foundation under Grant No. PHY-0354572, PHY0456890 and the NASA-Arkansas Space Grants Consortium Award ASU15154. The work of L.W. Chen is supported in part by the National Natural Science Foundation of China under Grant No. 10105008.

REFERENCES

- [1] J.M. Lattimer and M. Prakash, Phys. Rep., **333**, 121 (2000); Astr. Phys. Jour. **550**, 426 (2001); Science Vol. **304**, 536 (2004).
- [2] A.W. Steiner, M. Prakash, J.M. Lattimer and P.J. Ellis, Phys. Rep. **411**, 325 (2005).
- [3] RIA Theory Bluebook, RIA theory working group, www.orau.org/ria/RIATG
- [4] B.A. Li, C.M. Ko and W. Bauer, *topical review*, Int. J. of Modern Phys. E**7**, 147 (1998).
- [5] *Isospin Physics in Heavy-Ion Collisions at Intermediate Energies*, Eds. B.A. Li and W. Udo Schröder, Nova Science Publishers, Inc (2001, New York).
- [6] L. Shi and P. Danielewicz, Phys. Rev. C**68**, 064604 (2003).
- [7] M.B. Tsang et al., Phys. Rev. Lett. (2004) .
- [8] L.W. Chen, C.M. Ko and B.A. Li, Phys. Rev. Lett. **94**, 32701(2005).
- [9] B.A. Li, C.B. Das, S. Das Gupta, C. Gale, Phys. Rev. C**69**, 011603 (2004); Nucl. Phys. **A735**, 563 (2004).
- [10] K. Chen et al., Phys. Rev. **166**, 949 (1968); G. Alkhozov et al., Nucl. Phys. **A280**, 365 (1977); A. Bol et al., Phys. Rev. C**32**, 623 (1985); V. Grundies et al., Phys. Lett. **B158**, 15 (1985); P.W. Lisowski et al., Phys. Rev. Lett. **49**, 255 (1982); S.K. Charagi and S.K. Gupta, Phys. Rev. C**41**, 1610 (1990).
- [11] C.B. Das, S. Das Gupta, C. Gale and B.A. Li, Phys. Rev. C**67**, 034611 (2003).
- [12] I. Bombaci and U. Lombardo, Phys. Rev. C**44**, 1892 (1991).
- [13] D.H. Youngblood et al., Phys. Rev. Lett. **82**, 691 (1999).
- [14] J. Piekarewicz, Phys. Rev. C**69**, 041301 (2004).
- [15] G. Colo, N. Van Giai, J. Meyer, K. Bennaceur and P. Bonche, Phys. Rev. C**70**, 024307 (2004).

- [16] R.B. Wiringa, Phys. Rev. C**38**, 2967 (1988).
- [17] W. Zuo, L.G. Gao, B.A. Li, U. Lombardo and C.W. Shen, Phys. Rev. C**72**, 014005 (2005).
- [18] F. Sammarruca, W. Barredo and P. Krastev, Phys. Rev. C**71**, 064306 (2005).
- [19] G.R. Satchler, Chapter 9: Isospin Dependence of Optical Model Potentials, in *Isospin in Nuclear Physics*, page 391-456, D.H. Wilkinson (Ed.), (North-Holland, Amsterdam, 1969).
- [20] G.W. Hoffmann and W.R. Coker, Phys. Rev. Lett. **29**, 227 (1972).
- [21] P.E. Hodgson, The Nucleon Optical Model, pages 613-651, (World Scientific, Singapore, 1994).
- [22] A.J. Koning and J.P. Delarocje, Nucl. Phys. **A713**, 231 (2003).
- [23] J. Rizzo, M. Colonna, M. Di Toro and V. Greco, Nucl. Phys. **A732**, 202 (2004).
- [24] B.A. Li, Phys. Rev. C**69**, 064602 (2004).
- [25] B. Behera, T.R. Routray, A. Pradhan, S.K. Patra and P.K. Sahu, Nucl., Phys. **A753**, 367 (2005).
- [26] O. Sjöberg, Nucl. Phys. **A265**, 511 (1976).
- [27] Z.Y. Ma, J. Rong, B.Q. Chen, Z.Y. Zhu and H.Q. Song, Phys. Lett. **B604**, 170 (2004).
- [28] E.N.E. van Dalen, C. Fuchs and A. Faessler, Nucl. Phys. **A741**, 227 (2004); Phys. Rev. Lett. **95**, 022302 (2005).
- [29] J. Rizzo, M. Colonna and M. Di Toro, nucl-th/0508008.
- [30] J.W. Negele and K. Yazaki, Phys. Rev. Lett. **62**, 71 (1981).
- [31] V.R. Pandharipande and S.C. Pieper, Phys. Rev. C**45**, 791 (1991).

- [32] G.Q. Li and R. Machleidt, Phys. Rev. **C48**, 11702; *ibid*, **C49**, 566 (1994).
- [33] H.-J. Schulze et al., Phys. Rev. **C55**, 3006 (1997); A. Schnell et al., *ibid*, **C57**, 806 (1998).
- [34] D. Persram and C. Gale, Phys. Rev. **C65**, 064611 (2002).
- [35] G. Giansiracusa, U. Lombardo, and N. Sandulescu, Phys. Rev. **C53**, R1478 (1996).
- [36] M. Kohno, M. Higashi, Y. Watanabe, and M. Kawai, Phys. Rev. **C57**, 3495 (1998).
- [37] Qingfeng Li, Zhuxia Li, and Guangjun Mao, Phys. Rev. **C62**, 014606 (2000).
- [38] L.W. Chen et al., Phys. Rev. **C64**, 064315 (2001).
- [39] P. Danielewicz, Acta. Phys. Polon. B33, 45 (2002) and references therein.
- [40] F. Sammrruca and P. Krastev, nucl-th/0506081.
- [41] G.F. Bertsch, G.E. Brown, V. Koch and B.A. Li, Nucl. phys. **A490**, 745 (1988).
- [42] G.J. Mao, Z.X. Li, Y.Z. Zhuo, Y.L. Han and Z.Q. Yu, Phys. Rev. **C49**, 3137 (1994); G.G. Mao, Z.X. Li and Y.Z. Zhuo, *ibid*, **C53**, 2933 (1996); **C55**, 792 (1997).
- [43] T. Caitanos, C. Fuchs and H.H. Wolter, Phys. Lett, **B609**, 241 (2005).
- [44] M. Prakash, T.T. S. Kuo and S. Das Gupta, Phys. Rev. **C37**, 2253 (188).
- [45] S.A. Bass, J. Konopka, M. Bleicher, H. Stöcker and W. Greiner, GSI annual report, P66 (1994).
- [46] B.A. Li and S.J. Yennello, Phys. Rev. **C52**, R1746 (1995).
- [47] L.W. Chen, L.X. Ge, X.D. Zhang, and F.S. Zhang, J. Phys. G **23**, 211 (1997).
- [48] B.A. Li and C.M. Ko, Phys. Rev. **C57**, 2065 (1998).
- [49] A. Hombach, W. Cassing and U. Mosel, Euro. Phys. J. **A5**, 77 (1999).

- [50] J.Y. Liu et al., Phys. Rev. Lett. **86**, 975 (2001); Nucl. Phys. **A687**, 475 (2001); Phys. Rev. **C63**, 054612 (2001); Phys. Lett. **B540**, 213 (2002).
- [51] B.A. Li and S.J. Yennello, in *Isospin Physics in Heavy-Ion Collisions at Intermediate Energies*, Eds. B.A. Li and W. Udo Schröder, Nova Science Publishers, Inc (2001, New York).
- [52] F. Rami et al., Phys. Rev. Lett. **84**, 1120 (2000).
- [53] M. Prakash and K. S. Bedell, Phys. Rev. C **32**, 1118 (1985).
- [54] M. Lopez-Quelle, S. Marcos, R. Niembro, A. Bouyssy, and N. V. Giai, Nucl. Phys. **A483**, 479 (1988).
- [55] V. Baran, M. Colonna, V. Greco and M. Di Toro, Phys. Rep. **410**, 335 (2005).
- [56] M. Fujiwara, private communications.
- [57] J. Piekarewicz, private communications.
- [58] G. Colo, private communications.
- [59] A.W. Steiner and B.A. Li, nucl-th/0505051.
- [60] V.E. Starodubsky and N.M. Hintz, Phys. Rev. **C49**, 2118 (1994); B.C. Clark, L.J. Kerr and S. Hama, Phys. Rev. **C67**, 054605 (2003).
- [61] W. Reisdorf et al., Phys. Rev. Lett. **92**, 232301 (2004).
- [62] B.A. Li, P. Danielewicz and W.G. Lynch, Phys. Rev. **C71**, 054603 (2005).
- [63] W. Reisdorf, H.G. Ritter, Ann. Rev. Nucl. Part. Sci. **47**, 663 (1997); N. Hermann, J.P. Wessels and T. Wiedold, *ibid*, **49**, 581 (1999).
- [64] P. Danielewicz, R. Lacey and W.G. Lynch, Science **298**, 1592 (2002).
- [65] C. Fuchs, nucl-th/0505017.

- [66] G.F. Bertsch, W.G. Lynch and M.B. Tsang, Phys. Lett. **B189**, 384 (1987).
- [67] C.A. Ogilvie et al., Phys. Rev. **C42**, 10 (1990).
- [68] H.M. Xu, Phys. Rev. Lett. **67**, 2769 (1991).
- [69] V. de la Mota, F. Sebille, B. Remaud and P. Schuck, Phys. Rev. **C46**, 677 (1992).
- [70] G.D. Westfall et al., Phys. Rev. Lett. **71**, 1986 (1993).
- [71] D. Klakow, G. Welke and W. Bauer, Phys. Rev. **C48**, 1982 (1993).
- [72] B.A. Li, Phys. Rev. **C48**, 2415 (1993).
- [73] M.J. Huang et al., Phys. Rev. Lett. **77**, 3739 (1996).
- [74] B.A. Li, Phys. Rev. Lett. **85**, 4221 (2000).